Thermal Decomposition of Caffeic Acid in Model Systems: Identification of Novel Tetraoxygenated Phenylindan Isomers and Their Stability in Aqueous Solution

Richard H. Stadler,* Dieter H. Welti, Andreas A. Stämpfli,† and Laurent B. Fay

Nestlé Research Centre, Nestec Ltd., Vers-chez-les-Blanc, P.O. Box 44, CH-1000 Lausanne 26, Switzerland

Caffeic acid subjected to mild pyrolysis (225−226 °C) under vacuum resulted in rapid decarboxylation and the formation of simple catechol monomers as well as more complex cyclocondensed dimers and polymers. This reaction yielded the same spectrum of products as did acid-catalyzed cyclization of caffeic acid. The major pyrolysis products were identified by reversed-phase HPLC and LC−tandem mass spectrometry. Two novel compounds, identified by MS, ^{1}H NMR, and ^{13}C NMR as 1,3-*cis*- and 1,3-*trans*-tetraoxygenated phenylindans, were present as major products in both the caffeic acid pyrolysate and the acid-treated sample. The stability and reactivity of the pyrolysis products in weakly buffered aqueous solutions were determined concomitantly by measuring hydrogen peroxide generation and by monitoring the concentration of the individual components by reversed-phase HPLC. Such model studies may provide information pertaining to reaction mechanisms and the nature of the compounds involved in hydrogen peroxide formation in coffee.

Keywords: *Pyrolysis; caffeic acid; hydrogen peroxide; phenylindan isomers; model system studies*

INTRODUCTION

The formation of hydrogen peroxide in coffee solution over time has been unequivocally demonstrated by numerous investigators (Nagao *et al*., 1986a,b; Rinkus and Taylor, 1990; Tsuji *et al*., 1991; Stadler *et al*., 1994). Much emphasis has been placed on the relationship between hydrogen peroxide generation in coffee and the weak *in vitro* genotoxic effects that are observed in bacterial and mammalian mutagenicity test systems (Fujita *et al*., 1985; Itagaki *et al*., 1992). This contribution of hydrogen peroxide in coffee-mediated mutagenicity is undisputed, because *in vitro* mutagenicity can be effectively abolished by addition of antioxidative enzymes such as catalase or peroxidase (Nagao *et al*., 1986a; Friederich *et al*., 1985; Itagaki *et al*., 1992). Reports in this field have shown that dissolved oxygen and water temperature during coffee preparation are decisive factors in hydrogen peroxide formation. This may explain the large fluctuations in the levels of hydrogen peroxide reported in the literature (Fujita *et al*., 1985; Rinkus and Taylor, 1990; Stadler *et al*., 1994). The oxidative effects portrayed by coffee seem primarily attributed to polyphenolics which adventitiously form hydrogen peroxide when exposed to oxygen and metal catalysts. However, coffee and certain polyphenolic constituents can also act as potent antioxidants and antimutagens as shown in *in vitro* assays (Stich *et al*., 1982; Obana *et al*., 1986; Stich, 1991; Graf, 1992; Stadler *et al*., 1994), and coffee as a whole has also been reported to protect against various carcinogens in animal studies (Abraham, 1989; Aeschbacher and Jaccaud, 1990).

However, no detailed work has been done to elucidate the mechanisms and chemicals responsible for hydrogen peroxide formation and the antioxidative effects displayed by coffee. A report by Tsuji and co-workers showed that green coffee beans do not generate hydrogen peroxide, whereas roasted beans have this ability depending on the degree and duration of roasting (Tsuji *et al*., 1991). The same authors also propose the involvement of thermal decomposition products of caffeic acid, in particular the substituted benzenediol *p*-vinylcatechol. However, no data were presented that could confirm an active role of *p*-vinylpyrocatechol in hydrogen peroxide production either in model pyrolysis systems or in coffee itself. This dioxystyrene is apparently formed in trace amounts by decarboxylation of caffeic acid during pyrolysis or roasting (Clarke and MacRae, 1983; Heinrich and Baltes, 1987) and, as generally known for *o*- and *p*-dihydroxybenzene moieties, can produce hydrogen peroxide when exposed to atmospheric conditions (Clapp *et al*., 1990). Furthermore, this molecule is extremely susceptible to oxidation, resulting in rapid polymerization reactions in solution (Tiedke, 1936) and making isolation and identification difficult.

Even though caffeic acid has been implicated indirectly in the hydrogen peroxide generation process, there is only limited information on the ability of caffeic acid oxidation or pyrolysis products to produce hydrogen peroxide in model systems. Different pathways and products of chemically induced oxidation as well as autoxidation of caffeic acid at ambient temperatures have been described in the literature. The products of such reactions are diverse and include cyclolignans (Nahrstedt *et al*., 1990; Gumbinger *et al*., 1993), benzodioxane, and naphthalene-1,2-dihydro- (Cilliers and Singleton, 1991) and tetrahydrofuran-type compounds (Fulcrand *et al*., 1994). On the other hand, subjection of phenolic acids to thermal treatment results in rapid decarboxylation to furnish substituted styrenes (Klaren de Wit *et al*., 1971; Rizzi and Boekley, 1992) and simple vinylpyrocatechol monomers (Fiddler *et al*., 1967; Tsuji *et al*., 1991).

The positive correlation between the degree of roasting of the coffee beans and hydrogen peroxide formation suggests that the pertinent reductants are formed during roasting. To gain a better insight into the nature

* Author to whom correspondence should be addressed (fax +41/21 785 8553).

† Present address: Ciba-Geigy Ltd., K-127.5.02, 4002 Basel, Switzerland.

0021-8561/96/1444-0898$12.00/0

of the reducing components, one of the major catecholic constituents of green coffee, caffeic acid, was subjected to mild pyrolysis using model systems at temperatures employed during the actual roasting of coffee beans. Thus, the first objective of this work is to identify the major thermal degradation products of caffeic acid. Second, this study determines the contribution of the major individual pyrolysis products to hydrogen peroxide formation in a model system and assesses to what extent such model studies can reflect reaction mechanisms in a complex mixture such as coffee.

EXPERIMENTAL PROCEDURES

Chemicals. Chlorogenic acid and caffeic acid were purchased from Fluka (Buchs, Switzerland). Pyrocatechol was from Aldrich (Buchs, Switzerland). 4-Ethylpyrocatechol was from Lancaster (Strasbourg, France); homovanillic acid (HVA), horseradish peroxidase type II (HRPase), and quinic acid were obtained from Sigma (Buchs, Switzerland). All other reagents and solvents were of at least analytical grade purity.

Pyrolysis Procedures. Typically, 44.4 μmol of phenolic acid was heated on a heating module (Techne Dri Block DB-4) in a vacuum hydrolysis tube (5 mL volume) either evacuated (0.02−0.05 mbar) or under atmospheric conditions. Prior to pyrolysis under vacuum, water (30 μL) was added to create a slurry that enabled vacuum application without loss of material. Excess water was removed under vacuum at room temperature and the dry residue placed in the thermostated heater block preheated to 225−226 °C. After 15 min, the tube was removed and opened after reaching ambient temperature. The oily residue was taken up in 0.4 mL of a 50% methanolic solution and transferred into a beaker to which was added 40 mL of boiling potassium phosphate buffer (10 mM, pH 6.5). This solution (equivalent to 1.1 mM of caffeic acid as its pyrolysate) was then divided into two fractions each of 20 mL in separate beakers, to which was added $MnCl_2$ (1 mg/mL solution in water) to a give a final Mn^{2+} concentration of 2.2 μg/mL. The samples were then incubated at 35 °C in a thermostated water bath. Aliquots were removed for hydrogen peroxide determination (1 mL), HPLC, LC−MS, and LC−tandem mass spectrometry analyses as described.

Large-Scale Pyrolysis of Caffeic Acid and Isolation of Phenylindan Isomers. Caffeic acid (6 g, 33.3 mmol) was pyrolyzed in three consecutive 2 g lots under constant evacuation (0.08−0.3 mbar) for a period of 30 min using a Büchi GKR vacuum oven set at 230 °C. After pyrolysis was complete, the oily residue was left under vacuum to reach ambient temperature and then dissolved in methanol (10−20 mL) which was acidified with a few drops of dilute hydrochloric acid. The pooled residues were dried *in vacuo* (35 °C), affording 2.97 g of crude pyrolysate. Further purification was achieved by dissolving the pyrolysate in 10 mL of ether and loading the clear solution onto a silica gel column (80 g of silica gel 60, 70−230 mesh, Merck, Darmstadt, Germany) packed and preconditioned with ether. The column was eluted with ether, and fractions (20 mL) were collected manually. The phenylindan isomers were detected colorimetrically by removing aliquots (0.5 mL) of the ethereal effluent and adding one drop of 1 N NaOH. A very characteristic deep violet color developed due to phenylindan oxidation, which allowed simple and rapid detection of the phenylindan-rich fractions. This step afforded 0.4 g of the crude phenylindan isomer mixture with a purity as determined by HPLC analysis of approximately 65%. Yield based on a stoichiometry of 2 mol of caffeic acid affording 1 mol of phenylindan and 2 mol of CO_2 was in the range of 3−5.5% for both isomers together. A portion (150 mg, *ca.* 65% purity as determined by HPLC) of the crude phenylindan 1,3-*cis*/*trans* isomer mix was subjected to semipreparative HPLC using a Supelco LC-18 DB semipreparative column (10 × 250 mm) with solvent A (50 mM ammonium acetate, pH 4.0 with acetic acid) and solvent B (100% methanol), eluting isocratically with 45% solvent B for 20 min and then going to 55% solvent B immediately for a further 20 min at a flow rate of 2.0 mL/min. The compounds were detected photometrically eluting the *trans* isomer after $t_R = 36$ min and the *cis* isomer after $t_R = 37.1$ min. The peaks were collected manually and rechromatographed under the same HPLC conditions to ensure complete separation of the isomers. Thereafter, the fractions were concentrated *in vacuo* (35 °C) to remove methanol. Water and ammonium acetate were removed by lyophilization, affording 29 mg (0.11 mmol) the 1,3-*trans* (compound **I**) and 33 mg (0.12 mmol) of the 1,3-*cis* isomer (compound **II**), with a total yield of both isomers of 3.6%. The light orange powders of both the *cis* and *trans* isomers were then subjected to mass spectroscopic and NMR analyses as described.

Synthesis of the Phenylindan Isomers by Acid-Catalyzed Cyclization. Caffeic acid (1 g, 5.55 mmol) was suspended in 2 N sulfuric acid and refluxed for 2 h. The clear yellow solution was then cooled to room temperature and extracted into ether (3 × 30 mL). The organic layer was dried (solid Na_2SO_4), filtered, and concentrated *in vacuo* (40 °C) to afford 0.85 g of a gummy residue. Thin layer chromatography on silica gel plates (Merck, 60_{254}, 0.5 mm) with ether as developing solvent yielded 93 mg (0.34 mmol) of the phenylindan isomer mix ($R_f = 0.75$, visualized by UV at 256 nm or ammonia fumes). The 1,3-*cis*/*trans* isomers were purified by semipreparative HPLC employing conditions identical to those described in the previous section. Yields from 93 mg of the isomeric mixture after HPLC were 22 mg (0.081 mmol) of 1,3-*trans* isomer and 23 mg (0.085 mmol) of 1,3-*cis* isomer, giving a total yield of 5.9% for both isomers together.

Analytical HPLC Conditions. Analysis of the thermal decomposition products was carried out by HPLC employing a Waters 625 LC chromatograph system equipped with a Waters 994 photodiode array detector and a Waters 464 pulsed electrochemical detector, with both the UV and the electrochemical detectors interfaced to a Berthold HPLC program integrator. Samples were injected manually (50 μL). Separation conditions used a Supelco LC-18 DB column (4.6 × 250 mm, 5 μm) at a flow rate of 0.8 mL/min with a gradient going from 100% solvent A (5% acetonitrile in water with a total of 0.1% trifluoroacetic acid) after 10 min to 20% solvent B (100% acetonitrile with 0.1% trifluoroacetic acid) over 5 min, then to 40% B over 10 min, remaining at 40% B for 5 min, then to 50% B over 10 min, and finally to 100% B over 5 min. Compounds were detected photometrically (photodiode array detector range 200−400 nm) with wavelengths set at 220 and 280 nm. Electrochemical detection (ECD) was with a glassy carbon electrode with a working potential of 0.9 eV relative to the AgCl/KCl reference electrode. Pyrocatechol, 4-ethylpyrocatechol, and the tetraoxygenated phenylindan isomers in the pyrolysates were quantified by comparison of the peak integration area to a standard curve which was prepared by injecting different known amounts of stock solutions of the commercial standard compounds and the purified phenylindans (1, 5, 10, 20, and 40 μg/mL) under the same HPLC conditions as described above and integrating the UV signals at 220 and 280 nm.

Hydrogen Peroxide Measurements. Hydrogen peroxide was determined by the homovanillic acid/horseradish peroxidase (HVA/HRPase) assay initially reported for the measurement of activity of antioxidative enzymes (Guilbeault *et al.*, 1967; Snyder and Hendley, 1971). The dissolved pyrolysates (1 mL aliquots) were acidified with hydrochloric acid (1 M, 50 μL) and subjected to solid phase extraction on C_{18} Chromabond cartridges (500 mg, Macherey & Nagel, Düren, Germany), which were preconditioned with 2 bed-volumes each of methanol and water and finally 10 mM hydrochloric acid. After penetration of the pyrolysate solution, the columns were washed with 1 mL of 10 mM hydrochloric acid and the pooled effluents (2 mL total volume) analyzed for hydrogen peroxide content by the HVA/HRPase assay as described (Stadler *et al.*, 1994). Measurement of hydrogen peroxide generation of the individual peaks/regions isolated by semipreparative HPLC was done by collecting the fractions manually (2 mL) and removing excess acetonitrile under a stream of nitrogen at 35 °C for 15 min. Thereafter, a solution of boiling 50 mM potassium phosphate buffer (pH 6.5) was added to each of the

fractions to a final volume of 10 mL, to which was also added $MnCl_2$ to a final Mn^{2+} concentration of 2.2 μg/mL. Samples were incubated at 35 °C for 1 h. Aliquots (1 mL) were then loaded onto preconditioned C_{18} columns and the effluents analyzed for hydrogen peroxide content as described above.

Mass Spectroscopy. Electron impact (EI) and chemical ionization (CI) mass spectrometric measurements were carried out using a Finnigan MAT-8430 double-focusing mass spectrometer. EI spectra were recorded at 70 eV from 20 to 800 Da and positive CI spectra at 150 eV from 60 to 800 Da using ammonia as reagent gas. For both experiments the source temperature was 180 °C. The samples were directly introduced into the source of the mass spectrometer and heated at 2 °C/s. High-resolution measurements were made at a resolution power of 5000 using perfluorokerosene as reference compound. Silylation of the *cis* and *trans* isomers of the phenylindans was performed using a mixture of dimethylformamide/*N*,*O*-bis(trimethylsilyl)trifluoroacetamide (1:1 v/v) heated at 40 °C for 30 min and subsequent EI mass spectroscopy.

LC−MS and LC−MS/MS Analyses. Experiments were performed using a Finnigan TSQ-700 mass spectrometer connected via a thermospray interface to a Waters 600-MS pump and a Waters 717 autosampler. Separation was accomplished with a Macherey & Nagel C_{18} column (4.8 × 250 mm) operated at room temperature at a flow rate of 1 mL/min, starting at 100% solvent A (5% acetonitrile with 0.1% trifluoroacetic acid) for 10 min, then going to 20% solvent B (90% acetonitrile, 0.1% trifluoroacetic acid) over 5 min, then to 40% B over 10 min, remaining at 40% B for 5 min, then to 50% B over 5 min, and finally to 100% B over 5 min and resting at 100% B for 10 min. The thermospray was set at a discharge voltage of 1200 V, the vaporizer at 95 °C, and the source temperature at 260 °C, scanning over the mass range 50−600 Da. The collision gas was argon at 1.9 mTorr and a collision offset of 13.3 eV in the laboratory frame.

NMR Analyses. All measurements were performed on a Bruker AM 360 narrow bore spectrometer, using a 5 mm QNP quadrinuclear probehead at a ^1H frequency of 360.13 MHz and a ^{13}C frequency of 90.56 MHz or a selective 5 mm ^1H probehead. One-dimensional ^1H and proton-decoupled ^{13}C spectroscopy, ^1H homodecoupling experiments, NOE difference experiments, ^{13}C DEPT, and ^{13}C proton-coupled spectra with NOE, two-dimensional homonuclear proton correlation (COSY), $^1H-^{13}C$ heteronuclear correlation (HETCOR) optimized for a coupling of 145 Hz, and long-range heteronuclear correlation optimized for 8 Hz coupling were done for both phenylindans.

RESULTS

Hydrogen Peroxide Formation and HPLC Analysis of Caffeic Acid Pyrolysates. The first step in the analysis of the pyrolysates was to determine the hydrogen peroxide formation of a pyrolyzed caffeic acid solution over time. For comparative purposes, equimolar amounts of chlorogenic and quinic acid pyrolysis solutions were prepared under identical conditions as described (see Experimental Procedures) and the influence of Mn^{2+} on hydrogen peroxide formation determined. As depicted in Table 1, pyrolyzed caffeic acid catalyzed the highest levels of hydrogen peroxide formation over time. The same concentration of nonpyrolyzed caffeic acid incubated under the same conditions for 30 min produced 5 ± 0.8 and 9 ± 1.5 μM hydrogen peroxide (n = 4 ± SD) for caffeic acid solutions (does not fully dissolve in hot buffer at pH 6.5) without and with manganese addition (2.2 μg/mL), respectively. Therefore, manganese promotes autoxidation of both pyrolyzed and nonpyrolyzed caffeic acid but shows a much greater catalytic effect in the heat-treated phenolic acids. Furthermore, the chlorogenic acid pyrolysate fortified with manganese shows only about 25% of the hydrogen peroxide generating capacity as compared to equimolar amounts of the equally treated caffeic acid pyrolysate. Levels of hydrogen peroxide in quinic acid pyrolysates remained very low and did not increase over a time period of 1 h, with only a very minor increase in the same solution with added Mn^{2+}.

Table 1. Hydrogen Peroxide Formation[a] (Micromolar) of Pyrolyzed Chlorogenic Acids[b] over Time and Effect of Addition of Mn^{2+}

	caffeic acid		chlorogenic acid		quinic acid	
incubation time (min)	without Mn^{2+}	with Mn^{2+}	without Mn^{2+}	with Mn^{2+}	without Mn^{2+}	with Mn^{2+}
0	11 ± 1.3	15 ± 1.0	6 ± 1.2	16 ± 2.2	3.8 ± 0.8	11 ± 0.5
30	33 ± 2	104 ± 2	10 ± 3	24 ± 1	6 ± 0.5	15 ± 3
60	64 ± 2	205 ± 5	17 ± 1	41 ± 2	3.4 ± 0.3	18 ± 0.7

[a] Hydrogen peroxide determined by the HVA/HRPase method as described under Experimental Procedures. All incubations with the addition of a final concentration of 2.2 μg/mL Mn^{2+}. Entries are means ± SD (n = 4) of two independent experiments with duplicate determinations. [b] Pyrolysis of the acids under vacuum at 225−226 °C for 15 min; incubation (35 °C) in potassium phosphate buffer (10 mM, pH 6.5) at 35 °C. Detailed experimental conditions as described under Experimental Procedures.

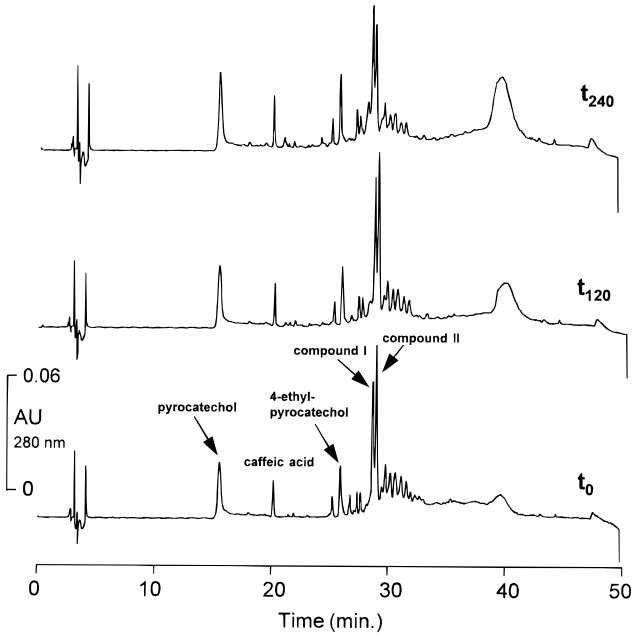

Figure 1. HPLC analysis (UV detection at λ = 280 nm) of vacuum pyrolyzed (225−226 °C, 15 min) caffeic acid dissolved in potassium phosphate buffer and incubated at 35 °C. Aliquots (50 μL) were injected, and hydrogen peroxide formation (HVA/HRPase assay) was determined concomitantly in the solution, revealing concentrations of 16, 350, and 480 μM hydrogen peroxide after t_0, t_{120}, and t_{240} min, respectively. Incubation and HPLC conditions are as described under Experimental Procedures.

The caffeic acid pyrolysate was subsequently analyzed by HPLC with dual UV and ECD without prior cleanup procedures. As portrayed in Figure 1, the thermal degradation products of caffeic acid which was pyrolyzed under vacuum at 225−226 °C for 15 min showed four prominent peaks in the HPLC trace (λ = 280 nm), the first two of which were identified as pyrocatechol (t_R = 15.4 min) and 4-ethylpyrocatechol (t_R = 26.1 min) by co-injection of standard compounds and on-line UV comparisons. The remaining two major components eluting after t_R = 29.1 and = 29.8 min were termed compounds **I** and **II**, respectively. These showed identical UV spectra, characteristic of substituted catechols (on-line λ_{max} = 286 nm) but with lack of the conjugated side chain (no absorbance at λ = 320 nm).

Table 2. Quantitation of the Major Caffeic Acid Pyrolysis Products[a] and Hydrogen Peroxide Production[b] of the Pyrolysate over Time

incubation time (min)	H_2O_2 formation (μM)	4-ethylpyro-catechol (μM)	pyro-catechol (μM)	compounds **I** and **II** (μM)
0	16	31	75	79
60	210	24	73	71
120	350	30	76	61
240	480	29	73	39

[a] Pyrolysis under vacuum at 225−226 °C for 15 min. Pyrolysate (obtained from 44.4 μmol of caffeic acid) dissolved in potassium phosphate buffer and reaction products quantified by HPLC analysis as described under Experimental Procedures. [b] Hydrogen peroxide determined by the HVA/HRPase method as described under Experimental Procedures. All entries are averages of duplicate determinations.

To elucidate the major compounds that could be involved in oxygen reduction, hydrogen peroxide measurements were performed after incubation times t_0, t_{120}, and t_{240} min, and the changes in the chemical composition of the pyrolysates were monitored simultaneously. As depicted in Figure 1, the weakly buffered pyrolysate products undergo prominent change in concentration over time. However, the amount of residual caffeic acid (t_R = 20.2 min) as well as pyrocatechol and 4-ethylpyrocatechol did not change significantly even after a 4 h incubation period (Table 2), with the level of hydrogen peroxide reaching up to 500 μM in the same pyrolysate solution. On the other hand, the levels of compounds **I** and **II** decreased rapidly over 4 h, with the concomitant increase in UV absorbing material eluting after 40 min. This polymeric material could not be identified further due to instability (polymerization) during purification attempts. The amount of hydrogen peroxide formed after the specified incubation times shows that the thermal reaction products eluting around t_R = 29−35 min contribute significantly to hydrogen peroxide formation. Therefore, the aforementioned monomeric 1,2-diphenols are not as susceptible as, for example, compounds **I** and **II** to oxidation and do not contribute significantly to hydrogen peroxide production in aqueous caffeic acid pyrolysates.

Caffeic acid that was thermally treated under atmospheric conditions at the same temperature and for the same duration of time as the vacuum pyrolysates showed the presence of the same degradation products but in different ratios. Analysis by HPLC (Figure 2) revealed higher levels of pyrocatechol and 4-ethylpyrocatechol but lower levels of compounds **I** and **II**, which were not easily distinguishable due to overlap of other reaction products in this region of the HPLC trace. As already observed (Figure 1), incubation of the atmospheric pyrolysate at 35 °C resulted in the rapid decomposition/polymerization of compounds **I** and **II** as well as the other electrochemically active products eluting in this region of the HPLC profile.

The apparent absence of polymeric material (which elutes as a broad region at t_R = 40 min) in the HPLC-ECD traces (Figure 2), which was clearly visible in the HPLC UV profiles after 4 h of incubation (Figure 1), is attributable to the lack of electrochemical activity of this material at the working electrode potential (0.9 eV). This polymeric material was clearly detectable at 280 nm and increased concomitantly with an increase in hydrogen peroxide levels as already observed for the vacuum pyrolysate. Comparison of the hydrogen peroxide generation revealed a 2-fold increase after the same incubation period as compared to the vacuum

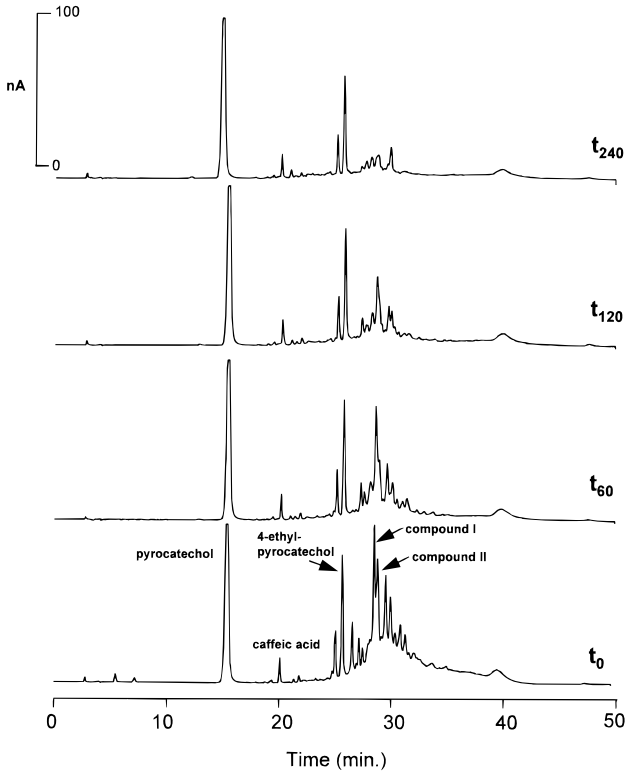

Figure 2. HPLC analysis (ECD) of caffeic acid pyrolyzed under atmospheric conditions (225−226 °C, 15 min), dissolved in potassium phosphate buffer and incubated at 35 °C. Aliquots (50 μL) were injected, and hydrogen peroxide formation (HVA/HRPase assay) was determined concomitantly in the solution, revealing concentrations of 88, 560, 725, and 900 μM hydrogen peroxide after t_0, t_{60}, t_{120}, and t_{240} min, respectively. Incubation and HPLC conditions are as described under Experimental Procedures.

pyrolysates. Furthermore, both pyrocatechol and 4-ethylpyrocatechol concentrations did not change significantly over 4 h, in contrast to the hydrogen peroxide level which reached up to 900 μM after the same time period. This again corroborates that hydrogen peroxide is not formed at the expense of monomeric benzenediols.

To assess the contribution of the individual pyrolysate reaction products to hydrogen peroxide generation, the crude pyrolysate obtained from 8.3 μmol of caffeic acid was injected onto a semipreparative HPLC column and all of the peaks/regions of the HPLC trace were collected manually (detection at λ = 280 nm). After removal of acetonitrile, hydrogen peroxide generation was measured after a 1 h incubation period (35 °C) in the individual fractions as described under Experimental Procedures. As portrayed in Table 3, compounds **I** and **II** contributed up to 56% of the total hydrogen peroxide formed in all of the collected peaks/regions together. The significantly lower contribution of pyrocatechol and 4-ethylpyrocatechol to hydrogen peroxide generation is therefore also demonstrated in the isolated compounds.

LC−MS and LC−MS/MS Analyses. The crude pyrolysate of caffeic acid was subjected to LC−MS, revealing the major pyrolysate products compounds **I** and **II** with identical base peaks of 163 Da. In the upper mass range there were no significant ions that could be attributed to the compounds of interest. The LC−MS/MS parent ion scan of the base peak ion at 163 Da gave a single ion at 273 Da, tentatively assigned to $[M + H]^+$ for both isomers, which were not well resolved under the HPLC conditions employed and eluted together as a relatively broad peak (see Experimental Procedures). An ion trace scan at *m*/*z* 407 Da revealed a smaller peak

Table 3. Hydrogen Peroxide Production[a] of the Major Pyrolysis Products of Caffeic Acid Isolated by Semipreparative HPLC[b]

compound/region	HPLC retention time (min)	H_2O_2 production (μM)
pyrocatechol	24.3	2.6
region A	31.8	2.1
region B	32.6	2.5
4-ethylpyrocatechol	33.7	16
region C	34−35.5	15
compound **I**	36	29
compound **II**	37.1	33
region D	37.2−41	10

[a] Hydrogen peroxide determined after an incubation period of 1 h at 35 °C in the presence of Mn^{2+} by the HVA/HRPase method as described under Experimental Procedures. All entries are averages of duplicate determinations. [b] Pyrolysate (225−226 °C for 15 min) derived from 8.32 μmol of caffeic acid. Peaks/regions were isolated by semipreparative reversed-phase HPLC as described under Experimental Procedures.

eluting *ca*. 1 min after compounds **I** and **II** that also showed an ion fragment at *m/z* 273 Da. This may be due to a more apolar higher molecular weight polymer consisting of three caffeic acid units, i.e. the cyclocondensation product of three 4-ethylene-1,2-dihydroxybenzyl moieties.

Minor peaks attributable to 4-ethylpyrocatechol and *p*-vinylpyrocatechol were also identified by their protonated molecular ions $[M + H]^+ = 139$ and $m/z = 137$, respectively. Daughter ion scans of the molecular ions of 4-ethylpyrocatechol gave $m/z = 123$ and 113 and for *p*-vinylpyrocatechol $m/z = 119$ and 100.

Characterization of Compounds I and II. The UV spectra of the purified compounds **I** and **II** were identical in all respects, with an absorption maximum at 285.5 nm in 10 mM HCl ($\log \epsilon = 3.74$), suggesting that these compounds are stereoisomers with loss of the caffeic acid conjugated side chain. Preliminary mass spectral results of both compounds obtained by LC−MS/MS of the crude pyrolysate revealed a base peak at $m/z = 163$ which, after a parent ion scan, resulted in a single ion at *m/z* 273. Identical mass spectral data were also obtained for both compounds in the EI mode, with molecular ions at $m/z = 272$ (M^+) and fragments at $m/z = 257$ $[M - CH_3]^+$, 255 $[M - OH]^+$, and 162 $[M - C_6H_5O_2]^+$ (Figure 3A). MS-CI revealed an $[M + NH_4]^+$ ion at 290 for compounds **I** and **II**. High-resolution mass spectrometry of the molecular ion gave $M^+ =$ 272.10507 amu and 272.10450 amu for compounds **I** and **II**, respectively. These values are in accordance with the theoretical value of 272.10486 amu and correspond to the molecular formula $C_{16}H_{16}O_4$. Silylation of both compounds **I** and **II** and subsequent EI-MS gave $M^+ =$ 560 for both isomers, with major fragmentation ions at *m/z* 545, 487, 471 $[M - OSi(CH_3)]^+$, 383, 307, 203, 147, and 73 $[Si(CH_3)_3]^+$, corroborating the presence of four silyl groups and suggesting a tetraoxygenated dimeric lignan derivative (Figure 3B).

Compounds **I** and **II** were procured by three different approaches, and each of the isomers was subjected to NMR investigation. The first approach was the initial small-scale pyrolysis, and the purified isomers were measured in DMSO-d_6 (proton spectra only). Thorough NMR analysis was done in the solvent CD_3OD (better solubility) on the products derived by sulfuric acid catalyzed cyclization. Third, NMR measurements were performed with the isomers obtained from the large-scale pyrolysis in both solvents to confirm the identity of the corresponding phenylindans. The ^1H and ^{13}C data

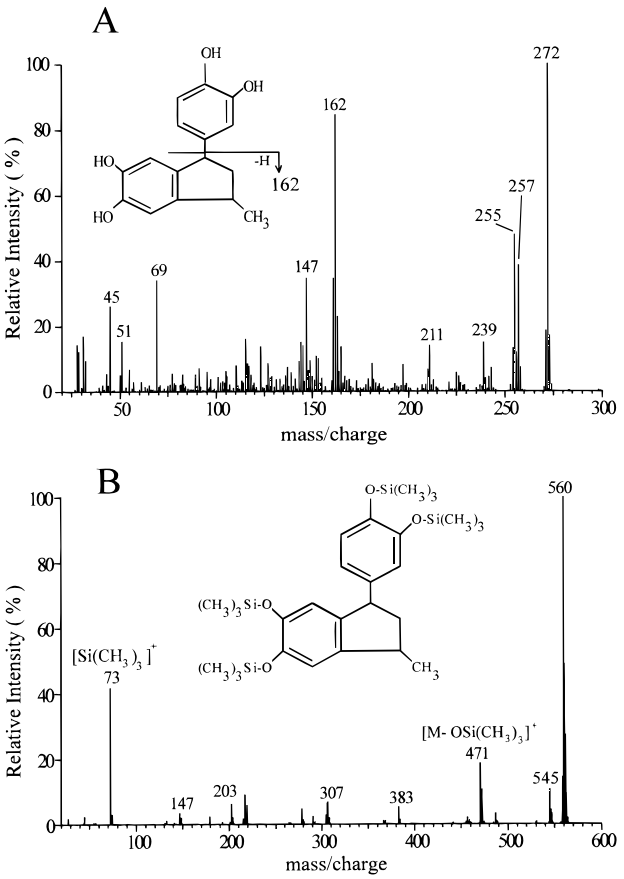

Figure 3. EI-MS spectra of (A) compound **I**, purified by semipreparative HPLC and (B) silylated compound **I**. Mass spectral conditions are as described under Experimental Procedures. Spectral characteristics of compound **II** were identical in all respects to those of compound **I** and are therefore not depicted.

Table 4. 360.13 MHz ^1H NMR Spectra[a] of 1,3-*cis*-[b] and 1,3-*trans*-Tetraoxy-1-methyl-3-phenylindans in CD_3OD

	1,3-*cis*		1,3-*trans*	
proton	ppm	multiplicity, J[c]	ppm	multiplicity, J[c]
1-H	3.002	m; J not extractable	3.176	6 lines, br; av J 6.6
2-H_α	1.428	d, t; 12.1, 10.4	2.040	d, d, d; 12.5, 8.1, 5.5
2-H_β	2.576	d, t; 12.1, 7.0	2.146	d, d, d; 12.5, 7.6, 6.0
3-H	3.925	d, d br; 10.5, 7.2	4.122	d, d sl br; 8.0, 6.1
4-H	6.148	d; 1.0	6.375	d; 0.9
7-H	6.631	d; 1.1	6.635	d; 0.8
8-CH_3	1.276	d; 6.7	1.188	d; 6.9
2′-H	6.593	d; 2.1	6.480	d, (d); 2.1, (?)
5′-H	6.691	d; 8.0	6.643	d; 8.0
6′-H	6.531	d, d, (d); 8.0, 2.1, 0.4	6.434	d, d, (d); 8.0, 2.1, 0.5

[a] Shift values in ppm, with TMS as an internal standard. Abbreviations: s = singlet; d = doublet; t = triplet; m = multiplet; av = average; sl = slightly; br = broad. [b] The *cis* compound could not be obtained pure; it always contained some *trans*-phenylindan (ca. 10%) and traces of a structurally related compound, possibly the ring-opened dimeric precursor of the *cis*/*trans* phenylindans. [c] Coupling constant(s) in Hz, absolute values, measured with at least 0.12 Hz/point resolution and moderate resolution enhancement. Coupling constants below 0.4 Hz are not listed.

in CD_3OD of compounds **I** and **II** obtained by acid-catalyzed cyclization are given in Tables 4, 5, and 6, respectively, the proton data correlating well with earlier results published on nonoxygenated phenylindans (Taylor *et al*., 1977). [NMR data of the *cis*/*trans*-phenylindans in DMSO-d_6 are available upon request (D.H.W.).]

Common features of both compounds in the ^1H NMR spectra were five aromatic proton signals in a pattern

Table 5. ^{1}H Homonuclear Coupling Constants (of at Least 0.4 Hz) of 1,3-*cis*- and 1,3-*trans*-Tetraoxy-1-methyl-3-phenylindans in CD_3OD

scalar coupling	1,3-*cis* (Hz)	1,3-*trans* (Hz)
$^2J_{2\text{-H}\alpha,2\text{-H}\beta}$	12.1	12.5
$^3J_{1\text{-H},2\text{-H}\alpha}$	10.4	5.5
$^3J_{1\text{-H},2\text{-H}\beta}$	7.0	7.6
$^3J_{1\text{-H},8\text{-CH3}}$	6.7	6.9
$^3J_{2\text{-H}\alpha,3\text{-H}}$	10.4	8.1
$^3J_{2\text{-H}\beta,3\text{-H}}$	7.0	6.0
$^3J_{5'\text{-H},6'\text{-H}}$	8.0	8.0
$^4J_{1\text{-H},7\text{-H}}$	1.1	0.8
$^4J_{3\text{-H},4\text{-H}}$	1.1	0.9
$^4J_{2'\text{-H},6'\text{-H}}$	2.1	2.1
$^5J_{3\text{-H},5'\text{-H}}$	0.4	0.5

Table 6. 90.56 MHz ^{13}C NMR Spectra[a] of 1,3-*cis*-[b] and 1,3-*trans*-Tetraoxy-1-methyl-3-phenylindans in CD_3OD

carbon	1,3-*cis*, (ppm, multipl)	1,3-*trans* (ppm, multipl)
1-CH	39.03, d	38.96, d
2-CH_2	48.45, t	46.78, t
3-CH	50.98, d	50.04, d
3a-C	139.71, s	138.73, s
4-CH	112.46, d	112.68, d
5-C-OH	144.95, s	145.16, s
6-C-OH	145.24, s	145.45, s
7-CH	110.57, d	110.99, d
7a-C	141.13, s	141.48, s
8-CH_3	20.15, q	21.33, q
1′-C	138.70, s	139.59, s
2′-CH	116.15, d	115.74, d
3′-C-OH	146.22, s	146.13, s
4′-C-OH	144.61, s	144.40, s
5′-CH	116.15, d	116.13, d
6′-CH	120.71, d	120.12, d

[a] Spectrum with TMS as an internal shift standard. Abbreviations: s = singlet (quaternary carbon); d = doublet (CH); t = triplet (CH_2); q = quartet (CH_3). [b] As in Table 4.

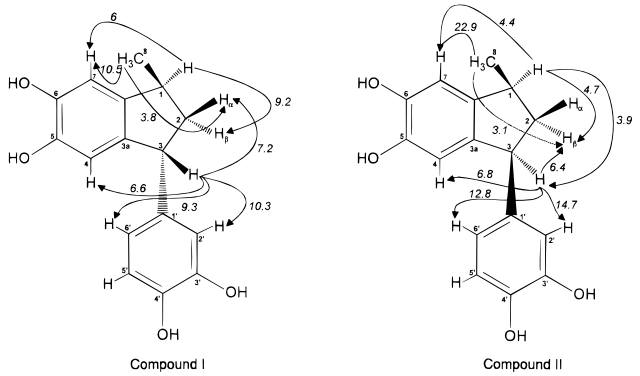

Figure 4. Structural formulas of compounds **I** and **II** showing the stereochemically significant proton nuclear Overhauser effects (in percent of the original signal intensity).

typical for two oxygen-bearing aromatic rings substituted at the 1-, 3-, and 4-, and the 1-, 2-, 4-, and 5-positions. Shifts and coupling topology of the aliphatic resonances were compatible with a five-ring fused to a benzene, with a second phenyl attached to one of the carbons directly bound to the first aromatic ring. In the small-scale pyrolytic products measured in DMSO-d_6, four slightly broadened phenolic OH signals could be observed in the range of 8.4−8.8 ppm but not individually assigned (*e.g.*, no COSY cross-peaks were seen for compound **I**). At higher concentration these four signals coalesced, and in CD_3OD they are not observed, due to exchange with the solvent. To clarify the NMR results, the global stereochemistry of compounds **I** and **II** is given in Figure 4. COSY cross-peaks and selective homodecoupling proved the couplings between 1-H and 7-H and between 3-H and 4-H, respectively. The facts that the proton shifts of 2-H$_\alpha$ and 2-H$_\beta$ are more different in compound **II** than in compound **I** and that the coupling constants of both 2-H to either methine proton are equal in compound **II** point to a *cis* configuration for this isomer. The most strategic of the NOEs observed in CD_3OD are illustrated by arrows in Figure 4. For compound **I**, they showed that the 8-CH_3, 2-H$_\alpha$, and 3-H hydrogens are all situated on the same side of the planes spanned by the five-ring. In compound **II**, the NOE from 8-CH_3 to 2-H$_\alpha$ is not observable because of the immediate vicinity of the two signals. The NOE of 3.1% from 8-CH_3 to 2-H$_\beta$ indicates that in the motion-averaged structure the 2-C atom must be above the approximate plane formed by carbons 1, 7a, 3a, and 3, bringing 2-H$_\beta$ upward. This is compatible with a 1-H,1-C,2-C,2-H$_\alpha$ torsion angle tending toward 180° and should reduce steric interaction between the 8-CH_3 and the 3-phenyl substituents. In the *trans* isomer (compound **I**), the proton shifts of 2-H$_\alpha$ and 2-H$_\beta$ are more equal and the coupling constants of 2-H$_\alpha$ (or 2-H$_\beta$) to the two methine protons are different. Those coupling constants seem to indicate a motion-averaged position of the 2-C atom close to the said plane, as corroborated by the absence of NOE from 8-CH_3 to 2-H$_\beta$.

The assignment of the protonated carbons was straightforward, while the quaternary carbons were identified by their long-range proton couplings (mainly three-bond) derived from long-range HETCOR experiments. For comparison, the ^{13}C spectrum of the phenylindans **I** and **II** was calculated by the STN Specinfo data base SPECAL prediction program (which does not take into account the stereochemistry), and reasonable correspondence with the measured spectra was observed (mean deviations of 4.0 and 3.8 ppm for *cis* and *trans*, respectively).

The results of the ^{1}NMR, ^{13}C NMR, and MS experiments confirm the structures of compounds **I** and **II**, respectively, as 1,3-*trans*-5,6-dihydroxy-3-(3′,4′-dihydroxyphenyl)indan-1-methyl and 1,3-*cis*-5,6-dihydroxy-3-(3′,4′-dihydroxyphenyl)indan-1-methyl, depicted in Figure 4.

Synthesis of Compounds I and II by Acid-Catalyzed Cyclization. Caffeic acid refluxed in 2 N sulfuric acid resulted in the formation of a very similar spectrum of compounds as compared to the pyrolytic procedure, revealing also compounds **I** and **II** as the main products with identical retention times and on-line UV spectra as their thermally generated counterparts. Both compounds **I** and **II** were present in *ca.* equal ratios and were purified by semipreparative HPLC to give overall yields in the region of 5−6% for both isomers. The 1,3-*cis* and 1,3-*trans* stereochemistry of the tricyclic dimers was corroborated by thorough NMR analyses.

DISCUSSION

Catechols (1,2-benzenediols) such as caffeic acid readily autoxidize in the presence of oxygen and transition metal catalysts to form reactive oxygen species which include the superoxide radical and hydrogen peroxide (Marklund and Marklund, 1974; Hanham *et al.*, 1983; Inoue *et al.*, 1992; Stadler *et al.*, 1995). The rate of formation of hydrogen peroxide is dependent on numerous factors, for example, oxygen tension, pH, ambient temperature, and transition metal availability. In particular, Mn^{2+} has been shown to catalyze the autoxidation of polyphenols and thus increase hydrogen

peroxide formation (Tyson and Martell, 1972; Inoue *et al.*, 1992; Stadler *et al.*, 1995), demonstrated here by the significant increase in the level of hydrogen peroxide in Mn^{2+}-fortified pyrolysis solutions of caffeic and chlorogenic acids.

The results presented here show that simple monomeric catechols such as pyrocatechol and 4-ethylpyrocatechol are not the major contributors to hydrogen peroxide formation in model pyrolysis systems, implicating dimers and higher molecular weight oligomers that are formed during cyclocondensation processes. Pyrolysis of caffeic acid under atmospheric conditions and under vacuum revealed the formation of novel 1,3-*cis*- and 1,3-*trans*-tetraoxygenated phenylindan isomers, which were progressively depleted over time with the concomitant formation of hydrogen peroxide. The amount of hydrogen peroxide formed in the pyrolysate solution shows that the phenylindans contribute only 17% of the total amount of hydrogen peroxide formed. This implies that the redox active oligomers/polymers of caffeic acid—eluting shortly after the phenylindans in the HPLC trace—also actively participate in the reduction of molecular oxygen.

It should be noted that the contribution of the phenylindans to hydrogen peroxide formation in the pyrolysate mixture is based upon their rate of decomposition, measured by analytical HPLC. However, the relative rate of hydrogen peroxide production of the isolated phenylindans, determined by measuring hydrogen peroxide directly in buffered solution, is much higher than in the pyrolysate mix (56 *vs* 17%). Thus, if redox recycling of the phenylindans occurs in the pyrolysate mix, then calculation of hydrogen peroxide evolution based solely on the loss of phenylindans will not reflect the true contribution of these compounds to the total amount of hydrogen peroxide formed.

It has been reported that in the presence of oxygen the thermal decomposition of ferulic acid (245 °C) is accelerated, leading to the incorporation of oxygen into thermal decomposition products (Fiddler *et al.*, 1967). The atmospheric pyrolysates of caffeic acid showed more products of oligomeric/polymeric nature as compared to thermal treatment under anoxic conditions. Oxygen can thus catalyze additional oxidative coupling reactions, leading to both a broader spectrum of products and the formation of more polymeric material.

Phenylindan-type compounds have been synthesized from styrene (Taylor *et al.*, 1977), propenylbenzenes such as isohomogenol and isosafrol (MacMillan *et al.*, 1969), and the dioxystyrene derivative cinnamic acid (Müller *et al.*, 1951). However, in the case of the latter, stereochemical characterization of the products was performed simply on chemical grounds and, to our knowledge, no such reactions have been reported for caffeic acid. The *cis*/*trans* phenylindan stereoisomers isolated from caffeic acid pyrolysates are thermal reaction products of caffeic acid, the latter having a proclivity to lose carbon dioxide readily due to tautomerization. The mechanistic route can be envisaged as a cyclization reaction of the reactive nucleophilic *p*-vinylpyrocatechol with a cation (Figure 5), as described for styrene (Taylor *et al.*, 1977; Rizzi and Boekley, 1992). The intermediary dimeric cation then eliminates a proton to cyclize intramolecularily to form the tricyclic dimer with 1,3-*trans* and 1,3-*cis* configuration in a *ca.* 1:1 ratio.

Naturally occurring phenylindan-type compounds termed sesquirins have been isolated from the redwood tree *Sequoia sempervirens* (Balough and Anderson, 1965, 1966). These compounds are responsible for the staining of the redwood and are structurally very similar to the phenylindan isomers isolated from the caffeic acid pyrolysates. Furthermore, the sesquirins have been proposed to function as precursors of more complex lignan structures (Balough and Anderson, 1966), also observed here for the phenylindan isomers which undergo rapid polymerization in the presence of atmospheric oxygen and transition metal catalysts.

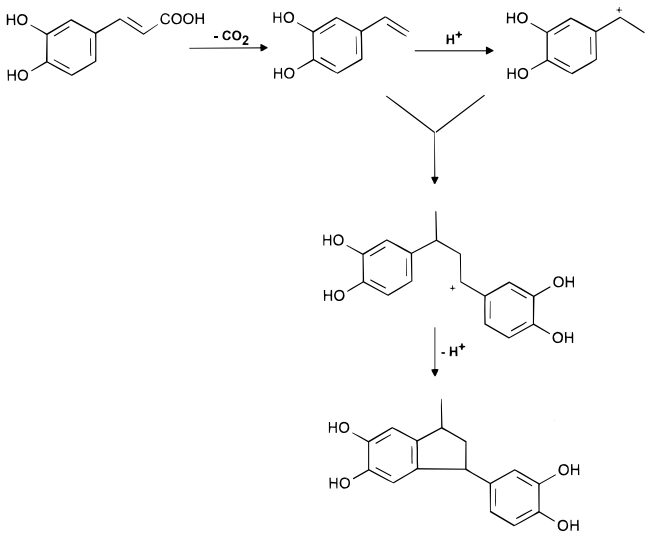

Figure 5. Proposed mechanism of formation of 1,3-*cis*- and 1,3-*trans*-phenylindans.

In food processing, model system reactions can give concrete ideas of possible reaction mechanisms, intermediates, and pathways. The incorporation of phenolic moieties that were derived from thermally treated ferulic acid into food macromolecules has been reported (Rizzi and Boekley, 1992). Moreover, analytical HPLC analysis with ECD of roasted and ground and instant coffees has shown that the *cis* and *trans* tetraoxygenated phenylindans described here are indeed present at levels ranging from 10 to 15 ppm (unpublished results). Even though such low levels of the phenylindans will not contribute significantly to the overall production of hydrogen peroxide in coffee, it is feasible that the reactive intermediates of caffeic acid pyrolysis interact with ambient nucleophilic functions such as sugars and amino acids. Curie point pyrolysis experiments with high molecular weight coffee melanoidins have already revealed the presence of covalently bound phenolics of phenylpropanoid origin (Heinrich and Baltes, 1987). Such complex oligomers of phenolic nature could undergo keto—enolization and redox cycling, leading to typical univalent reduction of molecular oxygen and formation of the superoxide anion radical. Dismutation of superoxide would thus generate hydrogen peroxide, a process typical for many di- and triphenolic compounds (Marklund and Marklund, 1974; Kahl, 1991). Therefore, in the case of coffee, hydrogen peroxide production is probably attributable to a plethora of diverse oligomeric and polymeric compounds, possibly with integrated catecholic moieties that readily autoxidize in the presence of oxygen and transition metal catalysts.

Preliminary *in vitro* data on the biological activity of the *cis*/*trans* phenylindans indicates that these tricyclic dimers display potent antioxidative and antimutagenic activity (Stadler, 1994; Guillot and Stadler, unpublished results). Further work is now underway to elucidate thermal degradation pathways of chlorogenic acids and

the interaction of pyrolysis products with other constituents in foods, as well as the potentially beneficial antioxidative effects of reaction intermediates and products.

ACKNOWLEDGMENT

We thank Ms. J. Richoz for excellent technical assistance and Mrs. F. Arce Vera for assistance with NMR spectroscopy.

LITERATURE CITED

Abraham, S. K. Inhibition of in vivo genotoxicity by coffee. *Food Chem. Toxicol.* **1989**, *27*, 787−792.

Aeschbacher, H. U.; Jaccaud, E. Inhibition by coffee of nitrosourea-mediated DNA damage in mice. *Food Chem. Toxicol.* **1990**, *28*, 633−637.

Balough, B.; Anderson, A. B. Chemistry of the genus *Sequoia*-II. Isolation of sequirins, new phenolic compounds from the coast redwood (*Sequoia sempervirens*). *Phytochemistry* **1965**, *4*, 569−575.

Balough, B.; Anderson, A. B. Chemistry of the genus *Sequoia*-III. Structural studies of isosequirin. *Phytochemistry* **1966**, *5*, 325−330.

Cilliers, J. J. L.; Singleton, V. L. Characterization of the products of nonenzymic autoxidative phenolic reactions in a caffeic acid model system. *J. Agric. Food Chem.* **1991**, *39*, 1298−1303.

Clapp, P. A.; Du, N.; Evans, D. F. Thermal and photochemical production of hydrogen peroxide from dioxygen and tannic acid, gallic acid and other related compounds in aqueous solution. *J. Chem. Soc., Faraday Trans.* **1990**, *86*, 2587−2592.

Clarke, R. J.; MacRae, R. *Coffee. Volume 1*: *Chemistry*; Elsevier Applied Science: London, 1983.

Fiddler, W.; Parker, W. E.; Wasserman, A. E.; Doerr, R. C. Thermal decomposition of ferulic acid. *J. Agric. Food Chem.* **1967**, *15*, 757−761.

Friederich, U.; Hann, D.; Albertini, S.; Schlatter, Ch.; Würgler, F. E. Mutagenicity studies on coffee: the influence of different factors on the mutagenic activity in the Salmonella/mammalian microsome assay. *Mutat. Res.* **1985**, *156*, 39−52.

Fujita, Y.; Wakabayashi, K.; Nagao, M.; Sugimura, T. Implication of hydrogen peroxide in the mutagenicity of coffee. *Mutat. Res.* **1985**, *144*, 227−230.

Fulcrand, H.; Cheminat, E.; Brouillard, R.; Cheynier, V. Characterization of compounds obtained by chemical oxidation of caffeic acid in acid conditions. *Phytochemistry* **1994**, *35*, 499−505.

Graf, E. Antioxidant potential of ferulic acid. *Free Radical Biol. Med.* **1992**, *13*, 435−448.

Guilbeault, G. G.; Kramer, D. N.; Hackley, E. A new substrate for fluorometric determination of oxidative enzymes. *Anal. Chem.* **1967**, *39*, 271.

Gumbinger, H. G.; Vahlensieck, U.; Winterhoff, H. Metabolism of caffeic acid in the isolated perfused rat liver. *Planta Med.* **1993**, *59*, 491−493.

Hanham, A. F.; Dunn, B. P.; Stich, H. F. Clastogenic activity of caffeic acid and its relationship to hydrogen peroxide generated during autooxidation. *Mutat. Res.* **1983**, *116*, 333−339.

Heinrich, L.; Baltes, W.; Vorkommen von Phenolen in Kaffee-Melanoiden (Occurrence of phenols in coffee melanoidins). *Z. Lebensm. Unters. Forsch.* **1987**, *185*, 366−370.

Inoue, S.; Ito, K.; Yamamoto, K.; Kawanishi, S. Caffeic acid causes metal-dependent damage to cellular and isolated DNA through hydrogen peroxide formation. *Carcinogenesis* **1992**, *13*, 1497−1502.

Itagaki, S. K.; Kobayashi, T.; Kitagawa, Y.; Iwata, S.; Nukaya, H.; Tsuji, K. Cytotoxicity of coffee in human intestinal cells in vitro and its inhibition by peroxidase. *Toxicol. in Vitro* **1992**, *6*, 417−421.

Kahl, R. Protective and adverse biological actions of phenolic antioxidants. In *Oxidative Stress: Oxidants and Antioxidants*; Sies, H., Ed.; Academic Press: London, 1991.

Klaren-de-Wit, M.; Frost, D. J.; Ward, J. P. Formation of *p*-vinylguaiacol oligomers in the thermal decarboxylation of ferulic acid. *Recueil* **1971**, *90*, 906−911.

MacMillan, J.; Martin, I. L.; Morris, D. J. Tricyclic dimers of propenylphenyl ethers-I. NMR and stereochemistry. *Tetrahedron* **1969**, *25*, 905−914.

Marklund, S.; Marklund, G. Involvement of the superoxide anion radical in the autoxidation of pyrogallol and a convenient assay for superoxide dismutase. *Eur. J. Biochem.* **1974**, *47*, 469−474.

Müller, A.; Toldy, L.; Halmi, G.; Meszaros, M. Dimeric propenyl phenol ethers. XII. The synthetic stereoisomer of diisohomogenol, diisoeugenol diethylether, and metanethole. *J. Org. Chem.* **1951**, *16*, 481−491.

Nagao, M.; Wakabayashi, K.; Fujita, Y.; Tahira, T.; Ochiai, M.; Sugimura, T. Mutagenic compounds in soy sauce, chinese cabbage, coffee and herbal teas. *Prog. Clin. Biol. Res.* **1986a**, *206*, 55−62.

Nagao, M.; Fujita, Y.; Wakabayashi, K.; Nukaya, H.; Kosuge, T.; Sugimura, T. Mutagens in coffee and other beverages. *Environ. Health Perspect.* **1986b**, *67*, 89−91.

Nahrstedt, A.; Albrecht, M.; Wray, V.; Gumbinger, H. G.; John, M.; Winterhoff, H.; Kemper, F. H. Structures of compounds with antigonadotropic activity obtained by *in vitro* oxidation of caffeic acid. *Planta Med.* **1990**, *56*, 395−398.

Obana, H.; Nakamura, S.; Tanaka, R. Suppressive effects of coffee on the SOS responses induced by UV and chemical mutagens. *Mutat. Res.* **1986**, *175*, 47−50.

Rinkus, S. J.; Taylor, R. T. Analysis of hydrogen peroxide in freshly prepared coffees. *Food Chem. Toxicol.* **1990**, *28*, 323−331.

Rizzi, G. P.; Boekley, L. J. Observation of ether linked phenolic products during thermal degradation of ferulic acid in the presence of alcohols. *J. Agric. Food Chem.* **1992**, *40*, 1666−1670.

Snyder, S. H.; Hendley, E. D. Sensitive fluorometric and radiomatric assays for monoamine oxidase and diamine oxidase. *Methods Enzymol.* **1971**, *17B*, 741−746.

Stadler, R. H. Phenylindans, their preparation and utilization. Eur. Pat. 94109355.1, 1994.

Stadler, R. H.; Turesky, R. J.; Müller, O.; Markovic, J.; Leong-Morgenthaler, P. M. The inhibitory effects of coffee on radical mediated oxidation and mutagenicity. *Mutat. Res.* **1994**, *308*, 177−190.

Stadler, R. H.; Markovic, J.; Turesky, R. J. In vitro anti- and pro-oxidative effects of natural polyphenols. *Biol. Trace Elem. Res.* **1995**, *47*, 299−305.

Stich, H. F. The beneficial and hazardous effects of simple phenolic compounds. *Mutat. Res.* **1991**, *259*, 307−324.

Stich, H. F.; Rosin, M. P.; Bryson, L. Inhibition of mutagenicity of a model nitrosation reaction by naturally occuring phenolics, coffee and tea. *Mutat. Res.* **1982**, *95*, 119−128.

Taylor, A. R.; Keen, G. W.; Eisenbraun, E. J. Cyclodimerization of styrene. *J. Org. Chem.* **1977**, *42*, 3477−3480.

Tiedke, C. Der Gerbstoffkomplex in Kaffee. *Z. Unters. Lebensm.* **1936**, *71*, 393−404.

Tsuji, S.; Shibata, T.; Ohara, K.; Okada, N.; Ito, Y. Studies on the factors affecting the formation of hydrogen peroxide in coffee. *J. Food Hyg. Soc. Jpn.* **1991**, *32*, 504−512.

Tyson, C. A.; Martell, A. E. Kinetics and mechanism of the metal chelate catalyzed oxidation of pyrocatechols. *J. Am. Chem. Soc.* **1971**, *94*, 939−945.

Received for review July 5, 1995. Accepted December 29, 1995.[⊗]

JF950411C

[⊗] Abstract published in *Advance ACS Abstracts*, February 15, 1996.